Heterodyne frequency measurements and frequency calibration standards for tunable diode lasers

J. S. Wells and F. R. Petersen

Time and Frequency Division, National Bureau of Standards, Boulder, Colorado 80303

and

A. G. Maki

Molecular Spectroscopy Division, National Bureau of Standards, Washington, DC 20234

Abstract

New frequency calibration tables are required to keep abreast of the resolution attainable by currently available tunable lasers. One key to the generation of tables with requisite accuracy involves accurate heterodyne frequency measurements; another key consists of reliable fitting and analysis. Coordinated activity in NBS involves selection of suitable molecular calibration candidates, their frequency measurement and analysis, and dissemination of the results in the form of frequency calibration tables. Current status of these efforts is described.

Introduction

Because tunable lasers afford a resolution some 100 times greater than the accuracy of available calibrations, a joint program (between the Time and Frequency Division in NBS Boulder Labs and the Molecular Spectroscopy Division in NBS, Gaithersburg) was initiated in 1978 to erect a network of secondary reference standards which would permit accurate calibration of tunable laser spectra. The objectives were to use the frequency measurement capabilities in NBS Boulder Labs to make precise frequency measurements on selected absorption lines of particularly well suited molecules and use the fitting and interpreting capabilities in the NBS Gaithersburg Labs to determine constants and provide interpolation. The accuracy objectives were an uncertainty of no greater than ±3 MHz. The best frequency calibration standards for tunable laser systems should satisfy the following criteria: (1) absorption lines (rather than laser or emission lines) will be used; (2) the absorbing gas must be convenient, i.e., must be readily obtained and easily handled; (3) there must be at least one calibration point every 0.5 cm^{-1} (additionally, several nearby spectral features to help identify the calibration line would be extremely valuable) (4) the lines must be well resolved and free of accuracy-limiting fine structure; and (5) each line must either be measured accurately or else calculated reliably and accurately. Although no single calibrant can fulfill these requirements over the entire spectral range, the requirements can be easily fulfilled in selected spectral regions by such linear molecules as OCS and N_2O. These two molecules cover a rather large region of interest in the 500 to 2300 cm^{-1} region. Gaps in the coverage of these two may be partially filled by other molecules such as CO or HCN. Some gaps in the OCS coverage are spanned by DBr, which has about 10 cm^{-1} gaps between pairs of lines, and thus does not meet criteria for the best standards; nonetheless, we have included it in our study since it spans a 350 cm^{-1} region.

In this paper, we will deal primarily with OCS since most of the heterodyne frequency measurements (HFM) for calibration tables have been made on that molecule. Three different labs have recently made measurements on OCS bands at 9.4 μm.[1-3] Both conventional tunable diode laser (TDL) measurements[4] and HFM contribute to new results at 11.6 μm[5,6] and new frequency measurements on the $^{13}CO_2$ laser were required to complete that work.[7] HFM on OCS have also been extended to the 5.8 μm region.[8] A great many more microwave measurements also contribute to the results we describe. These are sufficiently numerous that the interested reader should consult the original references cited at the end of this paper.

Tunable diode laser - CO_2 laser heterodyne techniques

A representative block diagram for tunable diode laser (TDL) - CO_2 heterodyne measurements is shown in Fig. 1. Either a liquid helium Dewar or a closed cycle cooler was used to refrigerate the TDL. The radiation from the TDL was collimated by a 5 cm F/1 ZnS polycrystalline lens. Off-axis parabolic mirrors were used to focus the TDL radiation on the entrance slit (S_1) of the monochromator and recollimate the beam after it emerged from the exit slit (S_2). For general use, the entrance slit was replaced with an aperture (which was blackened and shaped to reduce fringes due to slit reflections feeding back to the TDL), and another slit, typically 500 μm or greater, was used on the output.

The ZnSe beam splitter was used to divide the post monochromator collimated radiation. One beam was directed through a 50 cm long cell containing OCS and focused onto a PbSnTe photovoltaic detector. The other beam was sent through a 12.5 cm F/5 Ge focusing lens and mixed with the reference CO_2 laser beam in a HgCdTe detector/mixer having a 300 MHz 3 dB bandwidth. The detector was followed by a broadband IF amplifier (0.1-1200 MHz) with 25 dB gain. The output of the amplifier was fed to a spectrum analyzer, and the frequency of the beat signal was measured with a marker oscillator and frequency counter.

The CO_2 laser was stabilized to a saturated absorption dip in CO_2 (observed in fluorescence).[9] This laser was similar to those used in previous IR frequency synthesis experiments.[1] The estimated absolute fractional frequency uncertainty for the CO_2 laser is less than 2×10^{-10} which is negligible compared with other errors in these experiments. The CO_2 laser was focused onto the detector with a 40 cm focal length lens positioned to produce a beam waist at the mixer element. We estimate the CO_2 laser power at the detector to be about 1 mW.
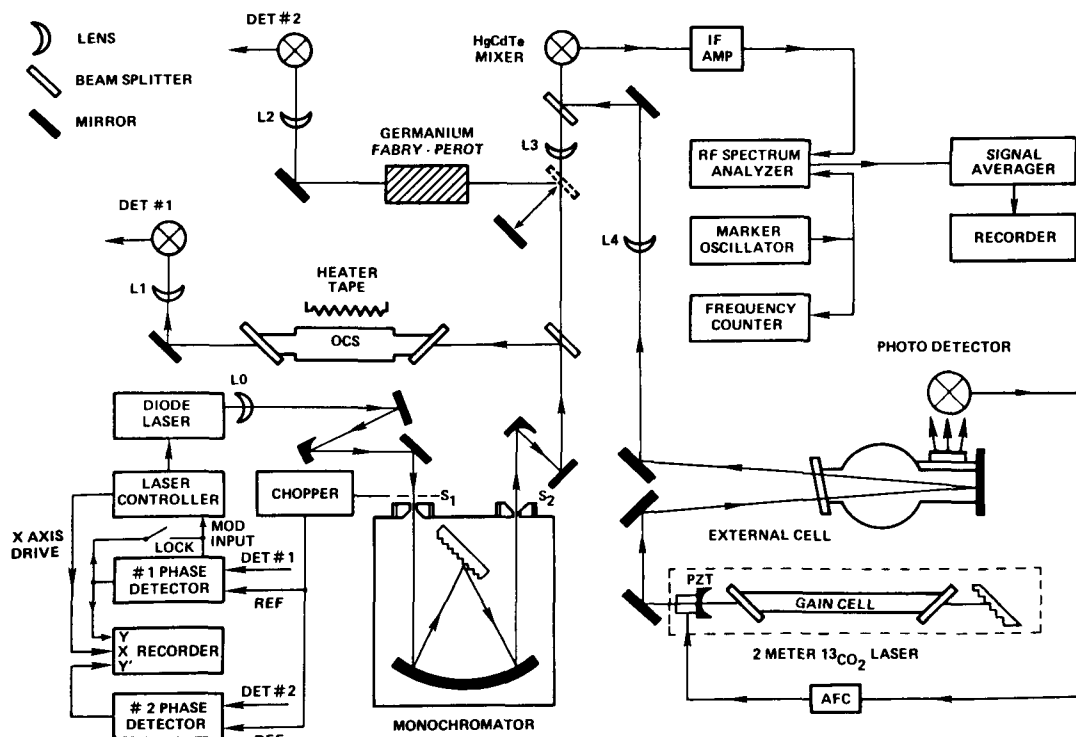

Fig. 1. Block diagram of scheme for TDL - $^{13}CO_2$ laser heterodyne frequency measurements.

The following procedure was used to minimize the error in locking the TDL to the absorption lines of interest. After the OCS line to be measured was identified, the monochromator was then adjusted to shape the transmitted TDL radiation so that it was nearly flat over the frequency region of the transition. (This procedure and a first derivative lock were used in lieu of a third derivative lock.) The chopper was then removed and the phase detector reference used to frequency modulate the TDL. The resultant first derivative signal was applied in proper phase to lock the TDL to the absorption feature of interest. In cases where the TDL mode slope made the monochromator adjustment impractical, an offset voltage was used in the servo loop to correct for a background slope. For the narrower linewidth TDL, a frequency modulation width of 10 MHz was used. For TDL with wider linewidths, attempts were made to avoid broadening the TDL linewidth by frequency modulation, subject to the condition that a suitable signal-to-noise ratio (S/N) for the derivative could be obtained.

After the CO_2 laser lock was verified, a marker oscillator was tuned to the center of the beat note and simultaneously fed to a frequency counter in order to measure the TDL-CO_2 laser difference frequency. The last step is needed because the beat notes observed thus far do not have sufficient S/N to drive a frequency counter reliably. The uncertainty in the frequency measurement is taken to be one-tenth of the beat note linewidth plus the frequency between derivative extrema divided by the S/N of the lock signal.

One spectral region of considerable interest is the 850-900 cm^{-1} region where nitric acid in the atmosphere can be detected by spectroscopic techniques. Since the 10^00-00^00 band of OCS can be used to calibrate this spectrum, a study of this band, as well as the 11^10-01^10 and 20^00-10^00 bands was made. The latter two bands provide additional calibration points in this region, and the Ritz combination principle permits calculation of the 20^00-00^00 band from the 20^00-10^00 and 10^00-00^00 band constants.

In order to make a reasonably good determination of the OCS constants, one would like (as a minimal goal) measurements which span the band center and extend in at least one branch to as high a value of J as possible. Use of the $^{13}CO_2$ laser barely permits this goal for normal OCS. Even so, it was necessary to construct a new $^{13}CO_2$ laser and to measure for the first time some hot band laser transitions to use as reference frequencies across the OCS band center. Fig. 2 shows the overlap of the $^{13}CO_2$ laser and the 11.6

µm OCS absorption band. The vertical lines indicate some close coincidences for potential heterodyne measurements. The solid part of the $^{13}CO_2$ laser curve represents the operable range of our 1.25 m stabilized CO_2 laser. When the $^{13}CO_2$ laser was stabilized, its frequency uncertainty was less than 0.2 MHz, and thus this frequency uncertainty was small compared to other possible contributions to uncertainty in the OCS frequency measurements shown in Table I. The dashed portion of the curve represents the extended range with an initially unstabilized 2 m higher gain laser. When the 2 m laser is used, we estimate that with great care one can tune its frequency to within about one MHz of the line center. For the key measurements involving the P(29) hot band laser transition, the 2 m laser was stabilized with an external absorption cell. The results of measurements on normal OCS are shown in Table I.
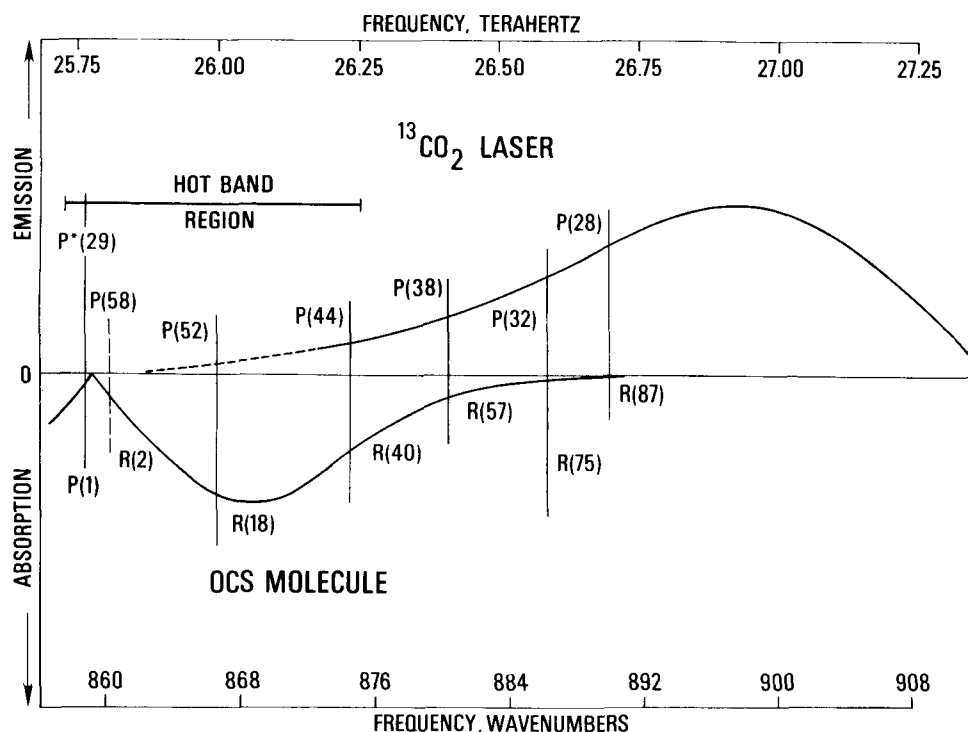

Fig. 2. Sketch of frequency overlap of $^{13}CO_2$ laser and OCS absorption band.

Table I. Frequencies of 11.5 µm Band Carbonyl Sulfide Absorption Lines Measured by the Heterodyne Technique.

Vibrational Transition	Rot. Trans.	OCS - $^{13}CO_2$ Meas. Freq. Diff. (MHz)	Measured OCS Freq. (MHz)[a]	Obs.-Calc. (MHz)
$10^00 - 00^00$	R(87)	+ 73.0	26 674 291.6 (6.0)	0.4
$10^00 - 00^00$	R(75)	+2773.8	26 566 226.9 (3.0)	-0.1
$10^00 - 00^00$	R(57)	+ 395.6	26 393 239.6 (2.0)	-0.1
$10^00 - 00^00$	R(40)	+1362.7	26 218 193.2 (3.0)	0.0
$10^00 - 00^00$	R(18)	+1733.6	25 975 344.4 (2.0)	-1.8
$10^00 - 00^00$	R(7)	-1668.0	25 847 177.1 (2.0)	1.5
$10^00 - 00^00$	P(1)	-1277.5	25 739 018.1 (2.0)	0.8
$11^1e_0 - 01^1e_0$	R(84)	+ 174.0	26 450 485.0 (3.0)	0.3
$11^1e_0 - 01^1e_0$	R(42)	- 628.4	26 034 711.5 (6.0)	0.2
$11^1e_0 - 01^1e_0$	R(25)	- 707.3	25 848 137.8 (2.0)	-0.7
$11^1e_0 - 01^1e_0$	R(22)	-1400.2	25 814 164.2 (2.0)	1.1
$11^1f_0 - 01^1f_0$	R(42)	+ 820.7	26 036 160.6 (6.0)	-1.0
$11^1f_0 - 01^1f_0$	R(25)	- 34.5	25 848 810.6 (4.0)	-0.2
$11^1f_0 - 01^1f_0$	R(22)	- 841.4	25 814 723.0 (4.0)	-1.9

Table I. Frequencies of 11. 5 μm Band OCS Absorption Lines Measured by the Heterodyne Technique (cont.).

Vibrational Transition	Rot. Trans.	OCS - $^{13}CO_2$ Meas. Freq. Diff. (MHz)	Measured OCS Freq. (MHz)[a]	Obs.-Calc. (MHz)
$20^00 - 10^00$	R(86)	+ 600.4	26 450 911.4 (3.0)	0.1
$20^00 - 10^00$	R(73)	- 439.6	26 334 336.9 (3.0)	-0.3
$20^00 - 10^00$	R(50)	+ 810.7	26 111 131.5 (4.0)	1.2
$20^00 - 10^00$	R(40)	+ 85.0	26 007 511.5 (4.0)	0.0
$20^00 - 10^00$	R(31)	- 329.0	25 910 930.4 (6.0)	2.3
$20^00 - 10^00$	R(16)	+2772.1	25 743 067.7 (3.0)	-0.7

a The estimated uncertainty (1-σ) in MHz is given in parentheses.

Table II. Heterodyne Frequency Measurements of Some Absorption Lines in the 10^00-00^00 Bands of Isotopic Species of Carbonyl Sulfide at 11.6 μm.

Molecular Species	Rot. Trans.	OCS - $^{13}CO_2$ Meas. Freq. Diff. (MHz)	Measured OCS Freq. (MHz)[a]	Obs.-Calc. (MHz)
$^{16}O^{12}C^{34}S$	R(89)	-2323.0	26 332 453.5 (4.0)	0.5
	R(63)	+2255.4	26 098 705.9 (2.0)	-0.5
	R(50)	-1602.6	25 972 008.2 (5.0)	0.5
	R(44)	+ 119.5	25 911 378.9 (3.0)	1.1
	R(38)	+ 558.0	25 849 403.1 (2.0)	-2.1
	R(35)	+2356.3	25 817 920.7 (2.0)	1.7
	R(28)	+2869.0	25 743 164.6 (3.0)	-0.3
$^{16}O^{13}C^{32}S$	R(90)	- 487.2	26 562 965.9 (5.0)	1.5
	R(71)	- 930.3	26 391 913.7 (4.0)	-0.8
	R(65)	+ 83.3	26 334 859.8 (6.0)	-2.3
	R(53)	- 338.1	26 216 492.4 (3.0)	-1.7
	R(45)	+ 899.4	26 134 476.3 (6.0)	0.5
	R(33)	- 548.5	26 006 878.0 (5.0)	3.0
	R(30)	+ 516.8	25 974 127.6 (2.0)	-0.2
	R(19)	+2349.2	25 851 194.3 (3.0)	1.0
	R(16)	+1325.4	25 816 889.8 (4.0)	-1.3
	R(14)	-1016.0	25 793 837.4 (6.0)	-2.4
	P(2)	+1108.8	25 592 036.1 (5.0)	0.7
$^{18}O^{12}C^{32}S$	R(92)	+1562.4	26 036 902.3 (7.0)	-1.5
	R(85)	+1251.4	25 978 653.6 (4.0)	1.0
	R(70)	-1036.6	25 847 808.5 (3.0)	-1.0
	R(58)	-2947.0	25 737 348.6 (2.0)	0.4
	R(43)	+1282.6	25 592 209.9 (5.0)	-0.4

a The estimated uncertainty (2-σ)in MHz is given in parentheses.

Since isotopic variants of OCS exist in fairly large natural abundances for some of the species, cali-bration tables should also have the transition frequencies for these species and relative intensities proportional to their abundances. This additional information provides a unique signature for each region of the spectrum. The $^{13}CO_2$ hot band laser was subsequently stabilized and heterodyne frequency measure-ments were made on several other species. Some of these results are shown in Table II.

Tunable diode laser-CO laser heterodyne techniques

The $20^0 0-00^0 0$ band of normal OCS was determined in part by the measurements previously described along with the Ritz combination principle. Additional information on OCS isotopes in the $20^0 0-00^0 0$ band (and subsequent calculations of $20^0 0-10^0 0$ band) prompted resurrection of initial efforts to make heterodyne frequency measurements with a CO laser. This is more complicated as is shown in Fig. 3. Since the CO laser does not lend itself to a stabilization scheme with the required accuracy, it was necessary to synthe-size a reference for the CO laser operating frequency. The apparatus for this synthesis included a metal-insulator-metal (MIM) diode, two stabilized CO_2 lasers, and an X-band klystron. The radiation from the CO laser, the two CO_2 lasers and the klystron all impinged on the MIM diode. The beat frequency, ν_B, which propagated from the MIM diode was equal to

$$\nu_B = \nu_{CO} - (\ell\nu_1 + m\nu_2 + n\nu_{\mu w}), \tag{1}$$

where ν_{CO}, ν_1, ν_2 and $\nu_{\mu w}$ are the frequencies of the CO laser, a $^{13}C^{16}O_2$ laser, a $^{12}C^{16}O_2$ laser and an X-band klystron, respectively. The harmonic numbers, ℓ, m, and n, can be either positive or negative integers. The beat signal, typically on the order of 100 MHz, was amplified and displayed on a spectrum analyzer. The CO laser was tuned to the midpoint between the two frequencies marking the disappearance of the beat signal as the CO laser was tuned across its gain bandwidth. Thus, the measurement is also a determination of the CO laser line frequency. Reference 8 summarizes some of the CO laser frequencies
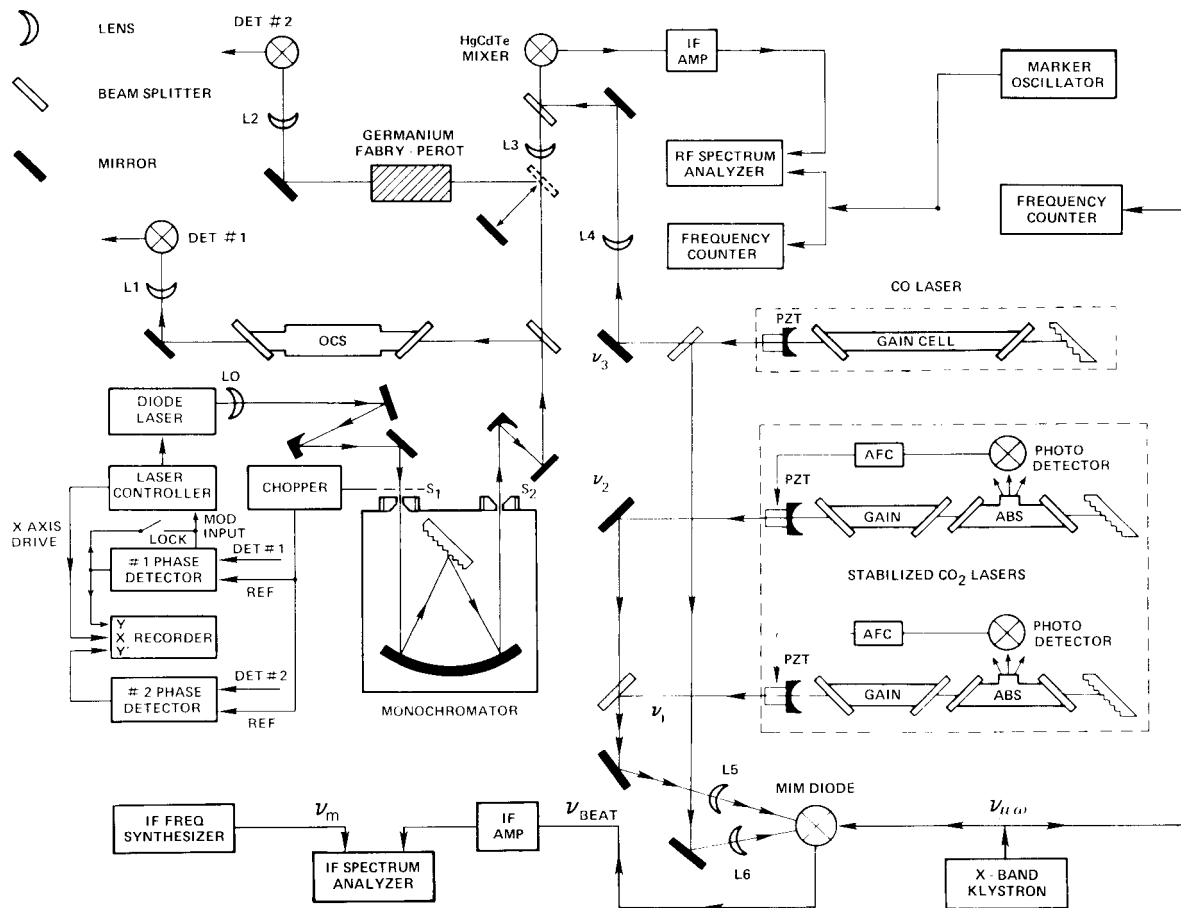

Fig. 3 Block diagram of scheme for TDL - CO laser heterodyne frequency measurements.

along with the CO_2 synthesis combinations used in the measurement. It should be emphasized, however, that the accuracy of the OCS measurement does not depend on locating the center of the CO lines since the CO laser frequency was manually adjusted to the measured value given in Reference 8 while the TDL - CO laser frequency differences were measured.

We note that the CO laser frequency values in the literature were typically 20-30 MHz different from our measured values; hence our measurements were essential in achieving our objective of obtaining an accuracy of ± 3 MHz for the OCS frequencies. Even so, we did not always meet this objective for individual measurements because of the TDL linewidth; however the data allow us to calculate many OCS frequencies with the desired accuracy.

The uncertainty in the 51 THz measurements resulted mainly from the TDL linewidth, where widths of tens of MHz were not uncommon. Again, the numerical value assigned to the uncertainty is essentially one tenth of the beatnote linewidth plus half the frequency between derivative extrema divided by the signal-to-noise ratio of the derivative signal. A much smaller contribution due to the frequency uncertainty of the reference laser is also included, but it was never greater than 0.2 MHz. Results of our first heterodyne frequency measurements at 51 THz are indicated in Table III.

Table III. Heterodyne Frequency Measurements Near 51 THz of the 20^00-00^00 Band Absorption Lines of Some Isotopes of Carbonyl Sulfide (OCS).

Molecular Species and Transition		CO Transfer Osc. Line	Measured Diff. $\nu_{ocs}-\nu_{co}$ (MHz)	Measured OCS Frequency[a] (MHz)		Obs.-Calc. (MHz)
$^{16}O^{13}C^{32}S$	P(34)	$P_{16}(12)$	-683.7	50 565 600.9	(6.0)	-1.8
	R(5)	$P_{15}(14)$	1082.5	51 089 622.8	(8.0)	-5.2
	P(9)	$P_{14}(20)$	3218.9	51 135 652.2	(7.0)	1.3
	R(15)	$P_{15}(13)$	1170.4	51 202 495.0	(10.0)	0.3
	R(20)	$P_{14}(19)$	4096.3	51 256 184.1	(6.0)	1.4
	R(31)	$P_{14}(18)$	-2972.2	51 367 804.0	(4.0)	-3.2
	R(58)	$P_{14}(16)$	-1879.4	51 603 367.6	(10.0)	4.9
	R(75)	$P_{14}(15)$	1920.4	51 722 938.5	(26.0)	5.1
$^{16}O^{12}C^{34}S$	P(5)	$P_{16}(12)$	1329.5	50 567 614.1	(4.0)	-1.2
	R(3)	$P_{16}(11)$	-1596.2	50 674 407.4	(6.0)	2.0
	R(44)	$P_{15}(14)$	-1510.0	51 037 030.3	(7.0)	-3.1
	R(58)	$P_{15}(13)$	-1638.3	51 199 626.3	(10.0)	-4.2
	R(65)	$P_{14}(19)$	-1582.8	51 250 505.0	(11.0)	1.0
$^{16}O^{12}C^{32}$	P(52)	$P_{16}(12)$	-1761.2	50 564 523.3	(10.0)	-1.3
	P(16)	$P_{15}(14)$	1857.9	51 090 398.2	(7.0)	-2.2
	R(27)	$P_{14}(16)$	-784.5	51 604 462.5	(6.0)	5.0
	R(39)	$P_{14}(15)$	-1258.3	51 719 759.8	(7.0)	1.1

a) A 2-σ estimated uncertainty in MHz is given in parenthesis.

Analysis and Fitting Techniques

A large quantity of data, in addition to the heterodyne frequency measurements, was used in the fitting process. We restrict our comments here to OCS. This is a molecule with a wealth of microwave measurement data, particularly for the normal molecule. Grating spectra were available for an overview; however these results were not used in the fitting. Measurements with a TDL and an etalon gave additional information on separations between OCS lines. Once a reliable calibration table was established for normal OCS, it was used to calibrate TDL spectra of the isotopes of OCS and to predict line positions for subsequent heterodyne frequency measurements. All of the data were given a weight proportional to the inverse square of the measurement uncertainty and then combined in the fitting process. The 20^00-00^00 band was calculated from

10^00-00^00 and 20^00-10^00 hot band results and the Ritz combination principle. The later hot band measurements spanned J=16 to J=86 as shown in Table I. Direct 20^00-00^00 band measurements shown in Table III spanned the band center, and all the data were refit. This iterative procedure culminated in the new constants used in the calibration atlas which is described below.

The data for the $\ell = 0$ states for each isotopic species were combined in a least-squares analysis based on the usual equations;

$$\nu_{obs} = \nu_0 + F'(J') - F''(J''), \text{ and} \tag{2}$$

$$F(J) = B_v J(J+1) - D_v J^2(J+1)^2 + H_v J^3(J+1)^3, \tag{3}$$

where, of course, $\nu_0 = 0$ was appropriate for the microwave transitions, and the H_v term was only used to fit the $^{16}O^{12}C^{32}S$ data. For $\ell=1$, the following equation was used instead of Eq. (3):

$$F(J) = B_v J(J+1) - D_v [J(J+1) - \ell]^2 \pm 0.5[q_v J(J+1) - q_{v,J} J^2(J+1)^2] \tag{4}$$

where the upper sign for the last term applies to the f levels and the lower sign to the e levels of the ℓ-doublet pair.

The reader is referred to the calibration atlas for the final values for the constants resulting from this work. Also included in that atlas is an analysis of the intensities which is outside the subject of this particular paper.

Status and availability of frequency calibration tables

Several molecules have been studied extensively and others have been studied on a limited basis. We list these below and indicate their coverage.

Carbonyl sulfide (multiband)

Tables of OCS absorption lines will be given for use as frequency calibration standards in the following regions of the infrared: 815-892 cm⁻¹, 1008-1092 cm⁻¹, 1649-1738 cm⁻¹, 1850-1921 cm⁻¹ and 2013-2140 cm⁻¹. The absorption line frequencies and approximate intensities are calculated from spectroscopic constants which have been determined by fitting selected data from the literature. This data includes heterodyne frequency measurements for all except the 2013-2140 cm⁻¹ region.[10] The uncertainties of most of the recommended frequency standards are on the order of 1 to 10 MHz. Hot band transitions and transitions for some of the less abundant isotopic species are included in the tables in order to provide patterns for the unambiguous identification of the lines as well as to provide additional calibration standards in some cases. The calibration atlas[11] contains over 6600 entries. (Prior to publication of the atlas, coverage of certain regions is obtainable by contacting one of the authors.) Table IV indicates the scope of the atlas, as far as the various bands and isotopes are concerned.

Table IV. Bands covered in tables 7 to 11 of the OCS Frequency Calibration Atlas.

Isotope	Vibrational	Band[a]	Table	ν_0(cm⁻¹)[b]
$^{16}O^{12}C^{32}S$	10^00-00^00	A	7	859
	$11^10-01^{1e}0$	B ⎫	7	852
	$11^10-00^{1f}0$	C ⎭		
	20^00-10^00	D	7	852
	$12^20-02^{2e}0$	E ⎫	7	846
	$12^20-02^{2f}0$	F ⎭		
	12^00-02^00	G	7	845
	$21^10-11^{1e}0$	H ⎫	7	846
	$21^10-11^{1f}0$	I ⎭		
$^{16}O^{12}C^{34}$	10^00-00^00	J	7	848
	$11^10-01^{1e}0$	K ⎫	7	841
	$11^10-01^{1f}0$	L ⎭		
	20^00-10^00	M	7	841
$^{16}O^{13}C^{32}S$	10^00-00^00	N	7	854
	20^00-10^00	O	7	847
$^{16}O^{12}C^{33}S$	10^00-00^00	P	7	853
$^{18}O^{12}C^{32}S$	10^00-00^00	Q	7	838

Table IV. Bands covered in tables 7 to 11 of the OCS Frequency Calibration Atlas (cont.).

Isotope	Vibrational	Band[a]	Table	ν_o(cm^{-1})[b]
$^{16}O^{12}C^{32}S$	02^00-00^00	A	8	1047
	03^10-$01^{1e}0$	B ⎫	8	1053
	03^10-$01^{1f}0$	C ⎭		
	12^00-10^00	D	8	1033
	04^20-$02^{2e}0$	E ⎫	8	1058
	04^20-$02^{2f}0$	F ⎭		
	04^00-02^00	G	8	1058
$^{16}O^{12}C^{34}S$	02^00-00^00	H	8	1045
$^{16}O^{12}C^{32}S$	20^00-00^00	A	9	1711
	21^10-$01^{1e}0$	B ⎫	9	1698
	21^10-$01^{1f}0$	C ⎭		
	30^00-10^00	D	9	1697
$^{16}O^{12}C^{34}S$	20^00-00^00	E	9	1689
$^{16}O^{13}C^{32}S$	20^00-00^00	F	9	1702
$^{16}O^{12}C^{32}S$	12^00-00^00	A	10	1892
	13^10-$1^{1e}0$	B ⎫	10	1892
	13^10-$01^{1f}0$	C ⎭		
	22^00-10^00	D	10	1872
$^{16}O^{12}C^{34}S$	12^00-00^00	E	10	1880
$^{16}O^{12}C^{32}S$	00^01-00^00	A	11	2062
	01^11-$01^{1e}0$	B ⎫	11	2055
	01^10-$01^{1f}0$	C ⎭		
	04^00-00^00	D	11	2105

a) Letter denotes vibrational band of a given isotope in the frequency table.

b) These approximate band center values are presented only to indicate the region covered. For the actual value of the band center and the reference from which it was obtained, refer to the atlas.[11]

Deuterium bromide (1-0 band), 1630-1985 cm^{-1}

Heterodyne frequency measurements have been made on selected deuterium bromide 1-0 band transitions ranging from P(20) to R(17). As in prior work, we measured the difference frequency beat notes between a tunable diode laser which was locked to the DBr absorption lines and a CO laser which was either locked or adjusted to a reference synthesized from CO_2 laser frequency standards. The beat note frequency was then combined with the CO laser frequency to give the DBr frequency. For two of the measurements, frequency doubled CO_2 laser radiation was substituted for the CO laser radiation. The measurements included electric quadrupole split triplets comprising the R(0) and P(1) transitions in the $D^{79}Br$ isotope. New DBr constants have been determined and a table of frequencies, believed to be accurate to 3 MHz, is available.[12] Separation between line pairs ranges from about 6 cm^{-1} at 1980 cm^{-1} to 11 cm^{-1} at 1630 cm^{-1} hence this molecule has limited utility. It does however, span the OCS gap between 1738 and 1850 cm^{-1} and partially covers another OCS gap between 1921 and 2013 cm^{-1}.

Carbon monoxide (2-0 band), 4120-4350 cm^{-1}

The 2-0 ro-vibronic band of $^{12}C^{16}O$ has been studied extensively by Fourier Transform Spectroscopy (FTS) techniques and has become a widely accepted calibration standard. Current developments with a color center laser (CCL) spectrometer have permitted use of an alternate technique not only to confirm these results, but also to lead to an improved set of molecular constants. A ring configuration CCL was locked to CO

absorption features and its frequency simultaneously measured relative to CO_2 laser frequency standards by heterodyning the CCL with appropriate harmonics of two CO_2 lasers. About 20 line center locks were made using a Doppler limited technique and involving J values up to 35. Subsequently, it was found possible to lock the CCL to 11 lines by observing the saturated absorption with a fluorescence technique, and some of the lower J lines were measured to an accuracy of better than 0.1 MHz. The data were combined in a least squares fit with seven unpublished microwave results to determine new constants which are an order of magnitude improved over prior results. A new frequency calibration table with some entries differing by as much as 15 MHz from FTS technique results will be available at the time of this conference.[13]

Nitrous oxide (multiband)

An interim table of N_2O frequencies covering 522 to 657 cm^{-1} and 1115 to 1340 cm^{-1} is currently in print.[14] Heterodyne frequency measurements were not available when the table was compiled and not many have been published at this time. Our next objective, however, is to compile a new N_2O frequency calibration atlas similar to that for OCS. Most phases of preparation are completed and we expect to start measurements this autumn.

References

1. Wells, J. S., Petersen, F. R. and Maki, A. G., "Heterodyne Frequency Measurements with a Tunable Diode Laser - CO_2 Laser Spectrometer: Spectroscopic Reference Frequencies in the 9.5 μm Band of Carbonyl Sulfide," Appl. Opt., Vol. 18, pp. 3567-3573. 1979.

2. Fayt, A., private communication, 1980.

3. Sattler, J. P., Worchesky, T. L., Maki, A. G. and Lafferty, W. J., "Heterodyne Frequency Measurements on Carbonyl Sulfide Near 1050 cm^{-1}," J. Mol. Spectrosc., Vol. 90, pp. 450-466. 1981.

4. Maki, A. G., Olson, Wm. B. and Sams, R. L. "High-Resolution Infrared Spectrum of the 859 and 1711 cm^{-1} Bands of Carbonyl Sulfide (OCS)," J. Mol. Spectrosc., Vol. 81, pp. 122-138. 1980.

5. Wells, J. S., Petersen, F. R., Maki, A. G. and Sukle, D. J., "Heterodyne Frequency Measurements on the 11.6 μm Band of OCS: New Frequency/Wavelength Calibration Tables for 11.6 and 5.8 μm OCS Bands", Appl. Opt., Vol. 20, pp. 1676-1684. 1981., and Erratum Appl. Opt. Vol. 20, p. 2874. 1981.

6. Wells, J. S., Petersen F. R., Maki, A. G. and Sukle, D. J., "Heterodyne Frequency Measurements (at 11.6 μm) on Isotopic Species of Carbonyl Sulfide, $OC^{34}S$, $O^{13}CS$, $OC^{33}S$, ^{18}OCS and $O^{13}C^{34}S$," J. Mol. Spectrosc., Vol. 89, pp. 421-429. 1981.

7. Petersen, F. R., Wells, J. S., Maki, A. G. and Siemsen, K. J., "Heterodyne Frequency Measurements of $^{13}CO_2$ Hot Band Transitions," Appl. Opt., Vol. 20, pp. 3635-3640. 1981.

8. Wells, J. S., Petersen, F. R. and Maki, A. G., "Heterodyne Frequency Measurements of Carbonyl Sulfide Transitions at 26 and 51 THz; Improved OCS, $O^{13}CS$ and $OC^{34}S$ Molecular Constants," J. Mol. Spectrosc., Vol. 98, pp. 404-412. 1983.

9. Freed, C. and Javan, A. "Standing-wave Saturation Resonances in the CO_2 10.6 μm Transitions Observed in a Low-pressure Room-Temperature Absorber Gas," Appl. Phys. Lett., Vol. 17, pp. 53-56. 1970.

10. Guelachvili, G., "Nombres D'ordes Absolus de la Bande ν_3 de $^{16}O^{12}C^{32}S$ par Spectroscopie de Fourier," Opt. Comm., Vol. 30, pp. 361-363. 1979.

11. Maki, A. G., Wells, J. S., Petersen, F. R., Lafferty, W. J., Olson, Wm. B., Fayt, A., and Sattler, J. P., "Tables of Carbonyl Sulfide (OCS) Absorption Line Frequencies and Wavenumbers for Calibration of Tunable Infrared Lasers," J. Phys. Chem. Ref. Data (in process).

12. Petersen, F. R., Wells, J. S., and Maki, A. G., "Improved Deuterium Bromide 1-0 Band Molecular Constants from Heterodyne Frequency Measurements," J. Mol. Spectrosc. (in process).

13. Pollock, C. R., Petersen, F. R., Jennings, D. A., Wells, J. S. and Maki, A. G., "Absolute Frequency Measurements of the 2-0 Band of CO at 2.3 μm, Calibration Standard Frequencies from Color Center Laser Spectroscopy," J. Mol. Spectrosc. (in press).

14. Olson, Wm. B., Maki, A. G., and Lafferty, W. J., "Tables of N_2O Absorption Lines for the Calibration of Tunable Infrared Lasers from 522 cm^{-1} to 657 cm^{-1} and from 1115 cm^{-1} to 1340 cm^{-1}," J. Phys. Chem. Ref. Data, Vol. 10, pp. 1065-1084. 1981.